Nov 24th, 12:00 AM

Experiments on Trapezoidal Steel Sheets in Bending

Allan Bergfelt

Bo Edlund

Hans Larsson

EXPERIMENTS ON TRAPEZOIDAL STEEL SHEETS IN BENDING

Allan Bergfelt[1] Bo Edlund[2] Hans Larsson[3]

SUMMARY

The behavior of thin-walled trapezoidal steel sheets under bending moment is studied. Experimental techniques are discussed. Attention is focused on evaluation of strain-gauge measurements (critical load determination and post-critical behavior) and on factors influencing the load carrying capacity (web buckling and load application).

1. INTRODUCTION

Cold-formed steel sheets of trapezoidal section are widely used for buildings in Sweden. The main consumption is for light industrial buildings. In the year 1973 about $5 \cdot 10^6$ m^2 of such sheet was used for roofs and about $3.5 \cdot 10^6$ m^2 for wall cladding of industrial buildings, which means about 80 per cent and 65 per cent respectively of the Swedish market for this application. In Sweden the design of thin-walled cold-formed sheets has, until recently, been based on the AISI Specification for the Design of Light Gage Cold-Formed Steel Structural Members (1). Since it was shown, however, that the load carrying capacity of sheets having low web buckling stresses may be overestimated by the method of the AISI-Specification (2),(3), new design rules were published by the Swedish government authorities in 1974 (4). In these rules the post-critical behavior of the web is taken into account by applying an effective width concept to the compressed part of the web.

---

1) 2) Professor and Associate Professor respectively, Division of Steel and Timber Structures, Chalmers University of Technology, Göteborg, Sweden.

3) Tekn.lic., Norrbotten Steel (NJA), Building Products Division, Luleå, Sweden ; formerly Research Assistant Div. Steel and Timber Struct., Chalmers Univ. of Technology, Göteborg, Sweden.

The aim of this paper is to present results and experiences from a number of experiments on transversely loaded thin-walled trapezoidal cold-formed steel sheets, some of which form the basis for the new Swedish rules (4). The sheets were simply supported and had various geometry and steel quality. The interest is mainly focused on an investigation carried out at Chalmers University of Technology (2), where 21 sheets with medium web slenderness ratio (d/t= = 110-125) were tested.

In section 2 a general discussion is given on the behavior of light gage steel beams in bending. This discussion is of an introductory character as is section 3, which deals with different aspects of experimental techniques. In sections 4 through 6 test results for different stages of beam behavior (critical, post-critical, and ultimate behavior) are presented.

2. BEHAVIOR OF THIN-WALLED TRAPEZOIDAL SHEET IN BENDING

This paper deals with cold-formed sheets having a type of cross section defined by Fig. 1. In the following a computational model will be used where the sheet is regarded as an assembly of initially plane plates having the widths a, b, and c respectively. With regard to buckling deformations the plates are treated independently of each other. Each individual plate is assumed to be simply supported along its longitudinal edges, which means that these edges can move only in the original plane of the plate. Thus the critical stress (bifurcation stress) of the flange plate, assuming long plate and elastic conditions, is

$$\sigma_{cr}^{a} = 4\,\pi^2\, E/12\,(1-\nu^2)\,(a/t)^2 \qquad (1)$$

and similar for the web plate :

$$\sigma_{cr}^{b} = k\pi^2\, E/12\,(1-\nu^2)\,(d/t)^2 \qquad (2)$$

Here ν is Poisson's ratio, E Young's modulus and k a buckling coefficient which is a function of the quotient $\psi = \sigma_e/\sigma_t$ between the edge stresses on the compression and tension side.

In the last equation d = b may be used, although d = h/sin θ has given better agreement with experiment.

The behavior of a light gage beam in bending is suitably described by the relationship between the bending moment M and the edge stress σ_e of the compression flange, Fig. 2.

According to the AISI-code the design of a light gage beam should be based on the engineering theory of bending extended by an effective width concept for the compression flange. For flange stresses below $0.46\,\sigma^a_{cr}$ the compression flange is regarded as fully effective. For higher stresses the width should be reduced to the effective width $a_e = [\,\alpha^{0.5} - 0.218\,\alpha\,]\,a$, where $\alpha = \sigma^a_{cr}/\sigma_e$. The moment at which the yield stress is attained in the compression (or tension) flange is regarded as the ultimate moment, which corresponds to point A of Fig. 2. Web buckling should also be checked using a rather high buckling coefficient k = 23.9, which sometimes leads to a critical edge stress smaller than the yield stress (point B in Fig. 2).

In most cases three different parts may be distinguished in the M-σ_e-diagram for the plate assembly model :

1) For small bending moments the full section is active - curve OD; the relationship is linear.
2) When the edge stress σ_e becomes larger than the critical flange stress σ^a_{cr} the effective width of the compression flange is reduced - curve DC ; the relationship is non-linear.
3) When the edge stress σ_e becomes larger than the actual critical stress of the web σ^b_{cr}, the effective width of the web will also be reduced - curve CF.

Point D in Fig. 2 corresponds to the moment M_D at which the reduction of the width of the compression flange begins. When the moment is further increased above M_D, the neutral axis of the beam will move towards the tension flange. This means that the compressed part of the web becomes larger and the critical stress of the web plate σ^b_{cr} decreases (curve D_1C). At a certain bending mo-

ment M_C (corresponding to point C of Fig. 2) the actual edge stress σ_e of the plate assembly model will be equal to the critical stress σ^b_{cr} of the web plate. For larger moments than M_C the initially plane web plate deflects and becomes only partly effective on the compression side (curve CF). When yielding has started in the compressed corner (point F) the local deformations rapidly increase and the structure finally fails by folding along one cross section.

3. EXPERIMENTAL PROCEDURE

3.1 Sheet geometry and material properties

It is important that the cross section geometry of each trapezoidal sheet is measured accurately. All dimensions shown in Fig. 1, which define the detailed cross section geometry, should be measured at a few sections of the sheet. Special equipment should be used to preserve the cross section geometry at least at the supports during the test (2). The wall thickness should be measured on the pure steel plate. If the sheet has zinc coating, small pieces are cut out from different parts of the sheet. The coating is then removed, e.g. with the aid of a hydrochloric acid solution ($HCl + SbCl_3$). In (2) the steel thickness variation within one sheet is only a few per cent. Therefore the average thickness of a sheet as determined from the total weight and surface may be used.
A systematic deviation from the ideal cross section geometry existing along the whole length of the sheet ought to be of interest also in those cases where the effect of initial out-of-flatness of the separate plates is not the purpose of the tests. For example: the whole compression flange may be curved in the transverse direction, which makes it act like a cylindrical panel, see section 4.

The yield stress σ_y and Young's modulus E of the sheet material are often determined by tension tests on strips cut in the longitudinal direction. In (2) all such tests were on 20 x 500 mm strips with zinc coating and the mechanical properties σ_y and E were evaluated disregarding the contribution of zinc in the composite zinc-steel material. Investigations at Cornell University (Karren, 1965 ; Uribe, 1969) have

shown that the yield stress for thin steel plates as determined from tension tests is a good and conservative approximation to the yield stress in compression.

3.2 Load application

The load is suitably applied as line loads at 2 or 4 sections of the simply supported sheet, c.f. Figs. 3 and 4. An arrangement with two loads is somewhat simpler and requires less loading equipment than a four-load-arrangement. In tests of pure bending strength, however, the two-load-arrangement may suffer from disturbances due to relatively large shear force and concentrated load at the ends of the pure-moment region.
The detailing of the loading pad (material selection and width of contact surface) has of course great influence on the web crippling load. The term 'web crippling' here denotes the localized buckling of the compressed part of the web under partial edge loading on the compression flange. Fig. 4a shows a test arrangement for the study of the interaction of bending moment and concentrated load.

The risk of web crippling is eliminated if the line load is applied to the tension flange through a 'bridge' with supports at every trough of the section.

A quite different solution of the loading problem is to apply an evenly distributed load using an air cushion or similar arrangement. This solution, however, should only be selected if there is a demand for the investigation of the interaction of plate and membrane action of the top flange of the beam. In this paper only 'free buckling' of the compression flange is discussed.

3.3 Deflection measurements

Deflections with respect to the supports are measured at midspan with inductance transducers or dial gauges. For determination of

the average beam deflection the transducers or gauges should be placed at the corners of the tension flange.
The relative deflection of a single compression flange plate measured with respect to the edges (corners) of the flange may also be of interest. Such measurements, however, require careful selection of the point (points) to be measured in order to enable a meaningful evaluation and interpretation of the results.

3.4 Strain measurements

In nearly all of the investigations where strains have been measured in thin-walled steel sheets a number of electrical resistant strain gauges were attached to the surface of the sheet at one cross section. Only a few authors report on the variation in longitudinal strain at different cross sections or on measurement of strain in the transverse direction (2, 5).
If the strain gauges are attached to one surface of the sheet only, it is hard to make a proper interpretation of the results. With a two-sided strain measurement membrane and bending strains may be separated. The experimentalist must be aware of the limitations and risks when studying strains at only one cross section, cf.(5).
The number of locations required for strain measurement in each cross section depends on the purpose of the test. For example the experiments reported in Reference 2 aimed at, among others, the determination of (1) the neutral axis of the cross section, (2) the edge membrane stress σ_e of the compression flange, and (3) the membrane and bending strains at the centre of the flange and web plates - all at the midspan section of the sheet. For this purpose 14 strain gauges were used in one 'wave' of the cross section, see Fig.5.

4. CRITICAL LOAD

The critical load of a light gage beam is here basically defined as (a) the transversal load or bending moment at the bifurcation point

of the corresponding perfect structure[1]. For the plate assembly model this corresponds to the smallest bifurcation load of any of the component plates. Practical trapezoidal steel sheets with unstiffened plates have such proportions that buckling nearly always starts in the compression flange. Therefore for such sheets the critical load may be alternatively defined as
(b) the bifurcation load of the compression flange plate. Due to elastic edge restraint from the webs this load may often be higher than the theoretical critical load of the simply supported flange plate in the plate assembly model.

As the basic definition (a) deals with changes in the behavior of the whole sheet regarded as a unit the critical load could – from a theoretical point of view – be determined as the limit load for the linear part of the load-deflection diagram. From a practical point of view, however, the definition of the experimental critical load used by Larsson (2) is more suitable since it enables a sharp determination from strain data in the following way : Measure the average membrane strain at the edges of both the compression flange ϵ_c (= average of strains at gauges no. 3, 5, 10, and 12 in Fig. 5) and the tension flange ϵ_t (from gauges no. 1, 7, 8, and 14). Compute the distance y from the compression flange to the neutral axis from the formula

$$y/h = \epsilon_c/(\epsilon_c + \epsilon_t) \qquad (4)$$

Then the bending moment at which the neutral axis starts to move away from the compression flange is defined as the experimental critical moment M_{cr}, see Fig. 6. A comparison of the values M_{cr} for the 21 sheets tested in Ref. 2 with the theoretical critical moment M_{cra} of the associated plate assembly model, corresponding to the critical stress of Eq. 1 , shows good agreement for all those sheets which have shapes of the kind used in current practice.

1) The differences in the behavior between the actual beam and the perfect one depends on the wavelength and amplitude of the initial imperfections.

For four beams with very wide tension flanges (c/t = 320-370) the ratio M_{cr}/M_{cra} was 1.1 to 1.3. Five beams had extremely wide compression flanges (a/t = 320-370) and probably also these flanges were initially deformed into a cylindrical panel, which could explain the high values of their experimental critical loads : M_{cr}/M_{cra} = 1.7 to 2.8. Another reason may be rather high restraint from the webs.
Thus, in contrast to the results of Rhodes and Harvey (6), the results of Ref. 2 show that for ordinary shapes of trapezoidal sheets there is no reason for using a larger value than 4 for the buckling coefficient in Eq. 1.

If the number of strain gauges is limited to two, the above definition (b) could be used. Then choose gauges no.4 and 11, see Fig.5, and place them as near the centre of the appearing buckle as possible. Determine the average strain $\epsilon_m = (\epsilon_{(4)} + \epsilon_{(11)})/2$. The following criterion ought to be efficient also for plates with relatively large initial imperfections (7) : The point on the load-strain curve (M- ϵ_m-curve) at which the compressive membrane axial strain ϵ_m at the centre of the plate has its maximum value (point m in Fig.7) is taken as an approximation of the critical load.

Hu et al.(8) have suggested another criterion, which only makes use of the strain data from the gauge on the convex side of the buckled plate. Here the load at the point of strain reversal of that gauge is used as a conservative approximation of the critical load of the plate (point s in Fig.7).

In comparison with the methods for single plates the criterion of neutral axis movement seems to be advantageous in many cases. The success, but also the limitation, of this method depends on the fact that the axial stiffness of an initially flat plate suddenly decreases to 40 to 60 per cent of its initial value, when the load passes its critical value. For imperfect plates the rate of this stiffness decrease becomes smaller when the amplitude of the initial deflection grows (7). Thus the method ought to be less sharp for plates with large initial deflections.

As mentioned above the critical load of an initially curved plate (cylindrical panel with radius of curvature R) is higher than that of the corresponding flat plate (7). This means that the critical moment M_{cr} of a trapezoidal sheet increases with the curvature parameter a^2/Rt of the compression flange plate. For a curved flange plate the buckling phenomenon is of a snap-through type characterized by a sudden jump in the axial strain at the centre of the flange plate, see Fig. 9. Note that in Fig. 9 the membrane strain ϵ_m drops after snap-through to approximately the level $\epsilon_{cr,0}$ of the critical strain for the corresponding simply supported flat plate.

However, curved plates with not too small curvature parameter, say $a^2/Rt > 40$, are imperfection-sensitive. In other words the buckling loads obtained in a test series of nominally equal curved plates have a large scatter due to small initial deviations from the perfect cylindrical form.

The writers are not aware of any investigation of the secondary effect of horizontal compressive forces in the transverse direction of the top flange induced by the sloping webs. Although this effect has very small influence on the critical moments discussed in this section, it may be of some interest in the discussion of ultimate loads, section 6.

5. POSTCRITICAL BEHAVIOR

In the following it is assumed that buckling starts in the flange. In the early postbuckling range of the plate assembly model only the compression flange plate is buckled (curve DC in Fig. 2). At point C also the web plate buckles and in the late postbuckling range both the compression flange and the compressed part of the web are participating only with their effective widths (curve CF). The length of the range CF depends mainly on the yield stress, the web slenderness parameter d/t and on the initial depth y_0 of the compression zone of the web. If for example y_0 is relatively small and the compression flange is wide the rate of increase in y after the flange has

buckled is rather great ; in such a case the critical web stress is rather high when the moment M is small, but after point D_1 in the diagram, Fig. 2, there will be a fast reduction of the critical web buckling stress due to the movement of the neutral axis.

It is believed that three parameters suffice for the classification of the postcritical behavior of light gage beams in bending, namely (a) the width-to-thickness ratio a/t of the compression flange, (b) the width-to-thickness ratio $y_0/t \sin\theta$ of the compressed part of the web in the full cross section (this parameter may be regarded as the product of the parameter y_0/h, which governs the buckling coefficient k in Eq. 2, and the web slenderness parameter d/t), and (c) the ratio $y_0/a \sin\theta$ between web and flange areas on the compression side, which also is the quotient between the second and the first parameter.
The parameter a/t determines the critical flange stress σ^a_{cr}. Eq. 1, and thus governs the critical moment $M_{cr} = W \cdot \sigma^a_{cr}$, which has a bearing influence on the length of the postcritical range – a beam with relatively small M_{cr} (i.e. small $M_{cr}/W\sigma_y$) is likely to have a long postcritical range. The parameter $y_0/t \sin\theta$ is decisive of the critical web buckling stress $\sigma^b_{cr,0}$ associated with the original, full section stress distribution. When $y_0/t \sin\theta$ is large, $\sigma^b_{cr,0}$ will be small and vice versa. The value of the combined parameter $y_0/a \sin\theta$ gives information on the rate of the reduction of the critical web stress in the early postbuckling range of the beam, i.e. after the flange has buckled. For example a large value of this parameter means that the critical web stress will decrease at a rather slow rate when the bending moment increases above M_{cr}.

The experimental determination of the $M-\sigma_e$-diagram may be made through strain-gauge readings at every loading step as was the case in Ref. 2, see for example Fig. 10. Let ϵ_c denote the average edge membrane stress of the compression flange, i.e. the mean from strain gauges no. 3, 5, 10, and 12, cf. Fig. 5. Then the stress $\sigma_e = E \cdot \epsilon_c$ is plotted versus the moment in the diagram, Fig. 10. Note that the strains were measured in the line B-B (centerline of the span) only. From the strain data in each loading step also the ratio y/h may be

computed, Eq.4, which gives the buckling coefficient k and the theoretical critical stress σ_{cr}^{b} (k) for the web plate, Eq.2, corresponding to the actual stress distribution. This method with $d = h/\sin\theta$ inserted into Eq.2 probably gives a somewhat conservative estimate of the critical web stress, because the width of the flat part of the web and the edge stress ought to be reduced due to the curved corners of the section.

Although the discussion of this section mainly deals with membrane strain it should be pointed out that the study of bending strain may also be worthwhile. For example in some tests of Ref.2 the bending strain at the centre of the flange and the web was found to increase rapidly at the critical load, cf. Figs.7, 8, and 9.

Measurements of strain in the transverse direction of the sheet are rare. In Ref.2 such measurements are reported for the top flange of one test. The results seem to support the assumption that the two longitudinal edges of each compression flange plate are not kept straight in the postcritical range but are free to pull in, i.e. they move towards each other in the region of the centre of a buckle. One evidence is that for the measured transverse membrane strain near the edge the approximate relationship $\epsilon_z \approx -\nu\,\epsilon_x$, ϵ_x being the axial membrane strain, holds, which indicates zero external stresses orthogonally to the edge ('stress-free' edge).
The periodic deformation of the initially straight corners between compression flange and webs induces deformations perpendicularly to the web but also vertical displacements of the corner if the tension flange is undisplaced.

Other changes in the shape of the cross section may take place under loading, for example a beam section consisting of three trapezoidal 'waves' may flatten out under the action of a line load, which means that the depth h and the angle θ of the web slope decrease locally. This type of deformation is mostly hampered by the friction of the loading beam.

It was already mentioned in section 4 that in tests into the early

postbuckling range the axial membrane strain in the centre of an initially curved compression flange was found to be approximately equal to the critical strain of the corresponding flat plate (i.e. the plate with the same width as the arc length of the curved plate). Experiments have also shown that the load versus edge strain curve of a curved plate, which is not too wide and not too curved, after snap-though approaches the postbuckling curve of the corresponding flat plate (7). Therefore, when evaluating experimental data, e.g. computing the ultimate load, the observed critical load for the curved plate should not be used in the formulas for load-carrying capacity, but should be replaced by the critical load for the corresponding flat plate.

6. LOAD CARRYING CAPACITY

The web buckling moment M_{crb} of a light gage steel beam discussed in the previous section (point C in Fig. 2) may be taken as a lower bound of the bending strength, provided the stress is below the yield stress. For the 21 sheets tested in Ref. 2 [1] the maximum moment obtained was 5 to 30 per cent greater than the predicted lower bound M_{crb}.

In the AISI Specification (1) the ultimate bending moment M_{ult} is computed as the moment at which the compression flange (edge) stress σ_e reaches the yield point σ_y (point A in Fig. 2) or at which the tension flange starts to yield ($\sigma_t = \sigma_y$). A formal web buckling moment M_{web} is also computed using Eq. 2 with k = 23.9, cf. Fig. 10. Then the smallest of the bending moments $M_{ult}/1.67$ and and $M_{web}/1.23$ is allowed. Although the 21 sheets of Ref. 2 have rather slender webs [1] the allowable moment according to this

1) The 21 trapezoidal steel sheets in Ref. 2 were loaded to failure with two line loads according to Fig. 3. The characteristic cross section parameters lie in the following intervals : d/t = 110-125, a/t = 30-370, c/t = 30-370 . Some sections were extremely unsymmetrical with the very wide flanges occurring either in the compression flange or in the tension flange, cf. Ref. 9.

method is governed by the moment M_{web} for 3 sheets only. When compared with the maximum moments M_{max} determined experimentally for this particular test series the ultimate moments M_{ult} predicted by the AISI-code were found to be too unconservative (2), cf. Fig. 10. In fact the actual failure loads were only 1.0 to 1.3 times the allowable loads according to the AISI Specification. Although the reason for the low failure loads in these tests may be some local effects in the neighbourhood of the concentrated line loads, see section 3.2, the results indicate, however, that the AISI Specification ought to be revised with respect to the ultimate load criteria for beams with slender webs. Possible ways of doing this may for example be to restrict the application of the simple method to beams with stocky webs (small d/t), to change the safety factors or to introduce a more accurate method for the computation of buckling loads of slender webs.

Another approach is to try to improve the prediction of ultimate moments by taking the postbuckling behavior of the web into account. Recently, different such approaches based on the plate-assembly model have been proposed (3, 4, 9, 10), which all aim at computing the load at incipient yielding (point F in Fig. 2). One approach uses a concave stress diagram on the compression side of the web, similar to the strain distribution found in tests. In most of these methods an effective-width concept is applied to the compression side of the web. For some of these approaches good agreement with the maximum loads of the tests of Ref. 2 was obtained (9, 10).

In order to increase the buckling strength of the web, designers have recently changed the web profile, Fig. 11.

The concentrated line load application in a bending test causes two kinds of disturbances which may reduce the failure load, cf. section 3.2 :

(a) web crippling of the region of the web just under the concentrated load, and

(b) buckling due to the combined effect of moment and shear in the

section just outside the constant-moment region ; further, in this section bending stresses are increased in wide-flange thin-walled beams due to shear lag.

A third disturbance occurs in sheets with sloping webs, where (c) the slope of the webs may have some influence on the local behavior in the neighbourhood of concentrated loads. Due to the slope the direct compressive stress transferred from the vertical load increases when the angle θ decreases. There is also a compressive stress induced into the top flange of the sheet in the transverse direction, which may reduce the load carrying capacity.

In nearly all the tests of Ref. 2 the failure mode was a local fold at either of the two line loads. With respect to web crippling, however, the failure loads were rather small - only 20 per cent of the crippling load according to the Swedish rules (4). On the other hand the maximum experimental moments were mostly 80 to 90 per cent (in three tests 95 per cent) of the ultimate moment computed by that variant of the 'total effective width' approach, which is recommended in Ref. 4.
It is possible that in the tested sheets of Ref. 2 the disturbance from large shear forces (shear lag) and direct external forces has caused some reduction in the load carrying capacity. The influence of such disturbance, which occurs at the interior supports of continous beams, may be studied by the 'moment-support' test shown in Fig. 4 a. The span length L in this test should be approximately 40 per cent of the length of each span of the prototype two-span beam in order to simulate the conditions at the central support of the prototype.

7. CONCLUSIONS

It has been shown in this paper that an idealized plate assembly model may be used for the analysis of thin-walled beams under pure bending. The model also facilitates the understanding of beam behavior.

Reference was given to a limited test series comprising 21 failure tests of trapezoidal steel sheets all having the web slenderness ratio $d/t \approx 115$. A number of experiences from this and other test series show the importance of proper determination of sheet geometry and material properties, of a suitable load application and of a careful selection of points for strain measurement.

It may be advantageous to define the load when the neutral axis starts to move towards the tension flange as the experimental critical load. It was found that the buckling coefficient $k = 4$ in Eq. 1 could be used for flange buckling in ordinary trapezoidal sheets. Some observed high critical loads could be explained by the initial form of the compression flange (cylindrical panel imperfection).

After the flange has buckled the theoretical critical stress of the web will decrease due to the shift of the neutral axis. The web buckling moment of the plate assembly model is a lower bound for the load carrying capacity in bending.
The behavior of a trapezoidal sheet in bending is suitably represented by a M-σ-diagram, Fig. 2. Three parameters govern the postcritical behavior of the sheet namely a/t, $y_0/t \sin \theta$, and $y_0/a \sin \theta$.

The results indicate that the method of the AISI-code ought to be modified for beams with slender webs. Recent approaches, which use an effective width both in flange and web, give failure loads which agree fairly well with experimental results.

ACKNOWLEDGEMENT

Part of this work was sponsored by the Swedish Council for Building Research (BFR).

REFERENCES

1. American Iron and Steel Institute, "Specification for the Design of Cold-Formed Steel Structural Members", AISI, New York 1968.

2. Larsson, Hans I., "Trapetsprofilerad stålplåt vid böjning" (Behavior of trapezoidal steel sheets in bending. In Swedish), Chalmers University of Technology, Dept. of Structural Engineering, Steel and Timber Structures, Report (Int. skr.) S 72:2, Göteborg 1972.

3. Thomasson, P.-O., "The influence of web buckling on the load carrying capacity of trapezoidal steel sheet sections (In Swedish)", Nordiske Forskningsdager for Stålkonstruksjoner (The Second Scandinavian Steel Structures Research Conference), Oslo 1973.

4. Statens Planverk, "Typgodkännanderegler No. 3", (The National Swedish Board of Urban Planning, Rules for general approvals No. 3. In Swedish). Stockholm 1974.

5. Pennington Vann, W., and Sehested, J., "Experimental Techniques for Plate Buckling", Second Specialty Conference on Cold-formed Steel Structures, St. Louis, Mo., Oct. 1973, Dept. of Civil Eng. Univ. of Missouri-Rolla, pp. 83-105.

6. Rhodes, J., and Harvey, J. M., "Alternative Approach to Light-Gage Beam Design", Journal of the Structural Division ASCE, Vol. 97, No. ST8, August, 1971, pp. 2119-2135.

7. Edlund, B., "Buckling and Postbuckling of Thin Rectangular Plates Under Longitudinal Compression", Chalmers University of Technology, Dept. of Structural Engineering, Report (Int. skr.) S 73:26, Göteborg 1973.

8. Hu, P.C., Lundquist, E.E., and Batdorf, S.B., "Effect of Small Deviations from Flatness on Effective Width and Buckling of Plates in Compression". NACA Technical Note No. 1124, September 1946.

9. Bergfelt, A.: "Profilés minces formés à froid". (Thin-walled cold-formed sections. In French). Bulletin Technique de la Suisse Romande, Vol. 99, No. 17, August, 1973, pp. 363-368.

10. Bergfelt, A., Edlund, B., and Larsson, H., "Web and Flange Buckling in Light Gage Steel Beams". Chalmers University of Technology, Internal Report S 75:8, Göteborg 1975.

APPENDIX - NOTATION

The following symbols are used in this paper :

a = width of compression flange ;

a_e = effective width of compression flange ;

b = flat width of web, see Fig. 1 ;

c = width of tension flange ;

d = clear distance between flanges measured along the plane of web ;

E = modulus of elasticity ;

h = depth of the beam section ;

k = buckling coefficient ;

M = bending moment applied to beam ;

M_{cr} = experimentally determined critical moment ;

M_{cra} = calculated buckling moment for the compression flange ;

M_{crb} = calculated buckling moment for the web ;

M_{max} = maximum moment determined experimentally ;

M_{ult} = ultimate moment according to the AISI Specification, Ref. 1 ;

M_{web} = web buckling moment according to AISI Specification, Ref. 1 ;

t = thickness of steel sheet (zinc coating removed) ;

W = section modulus;

y = distance from compression flange to neutral axis ;

y_0 = value of y at small loads ($M \approx 0$) ;

ϵ = experimentally determined strain ;

ϵ_c, ϵ_t = strain at the compression and tension side of the web respectively ;

ϵ_m = average membrane strain at centre of compression flange ;

θ = angle defining slope of web, Fig. 1 ;

σ_{cr}^{a} = critical stress in compression flange, Eq. 1 ;

σ_{cr}^{b} = critical compression stress in web, Eq. 2 ;

σ_t = stress in tension flange ;

σ_e = edge stress, stress on the effective width of the compression flange ;

σ_y = yield stress ;

ν = Poisson's ratio ;

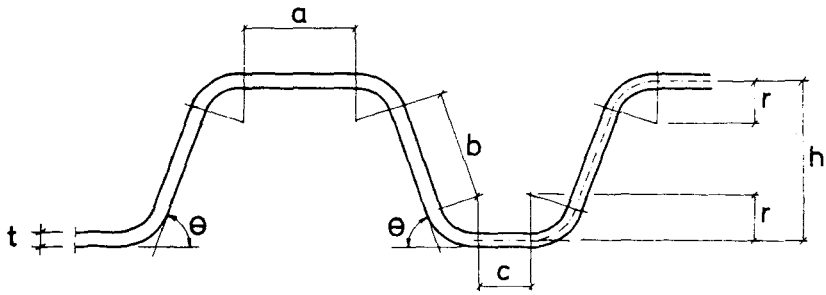

FIG. 1 CROSS SECTION DIMENSIONS OF STEEL SHEET.

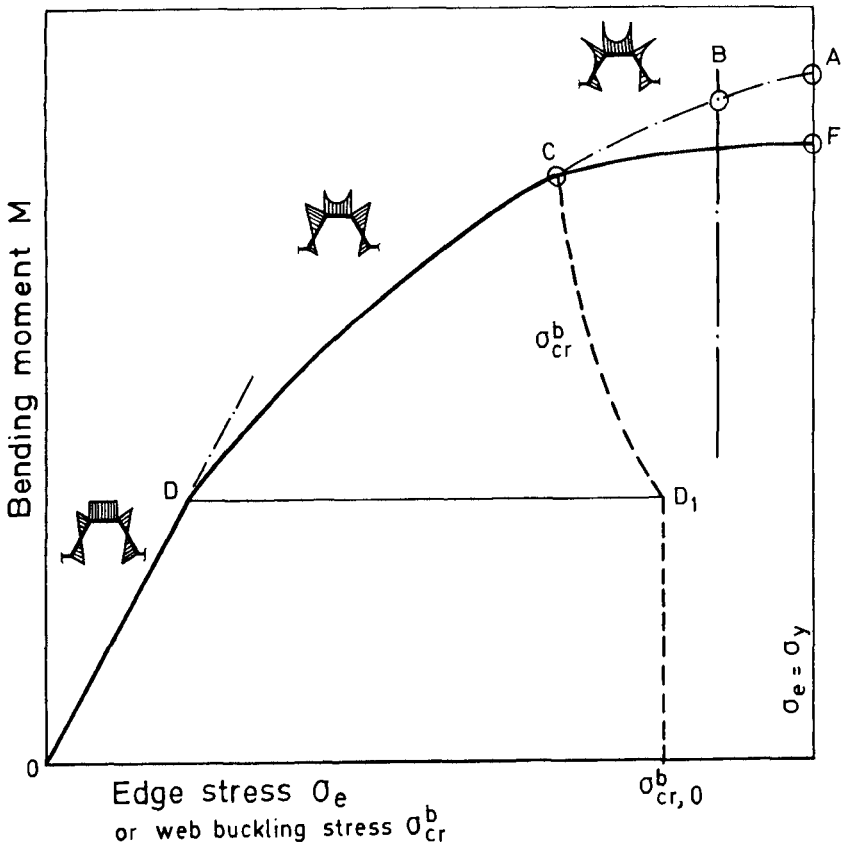

A is the ultimate moment calculated according to the AISI-code (M_{ult})

B is the web buckling moment calculated according to the AISI-code (M_{web})

C is the calculated moment for web buckling considering shift of neutral axis ($M_{c\,l\,b}$)

D is the critical moment for the compression flange

F is the calculated ultimate moment with reduced web

FIG. 2 MOMENT VERSUS EDGE STRESS RELATIONSHIP FOR THIN-WALLED BEAMS. WEB BUCKLING CRITERIA.

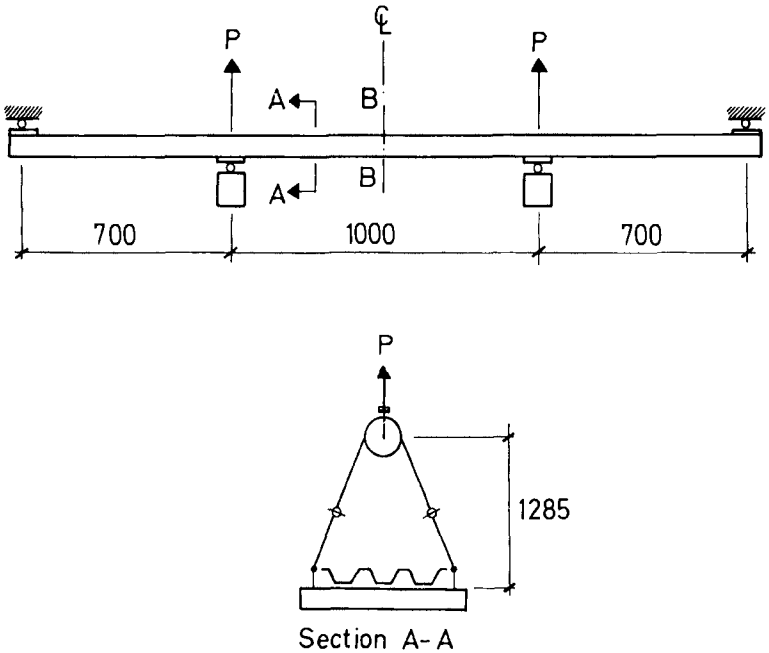

FIG.3 TESTING ARRANGEMENT FOR STEEL SHEETS.

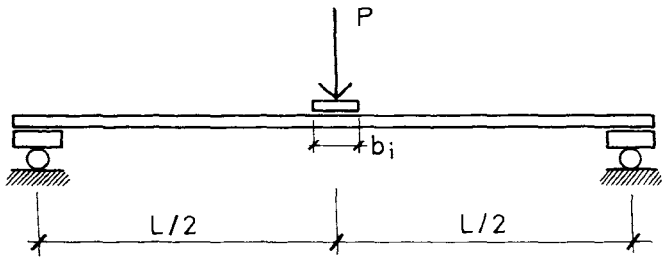

Moment-support test

(a)

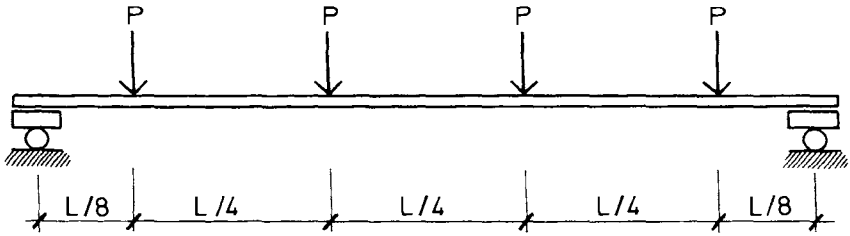

Moment-test

(b)

FIG.4 TESTS REQUIRED BY THE RULES OF THE NATIONAL SWEDISH BOARD OF URBAN PLANNING (4).

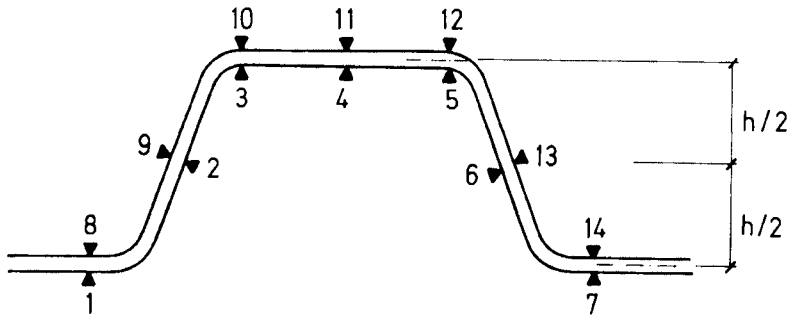

FIG.5 LOCATION OF STRAIN GAUGES IN LINE B-B OF FIG.3.

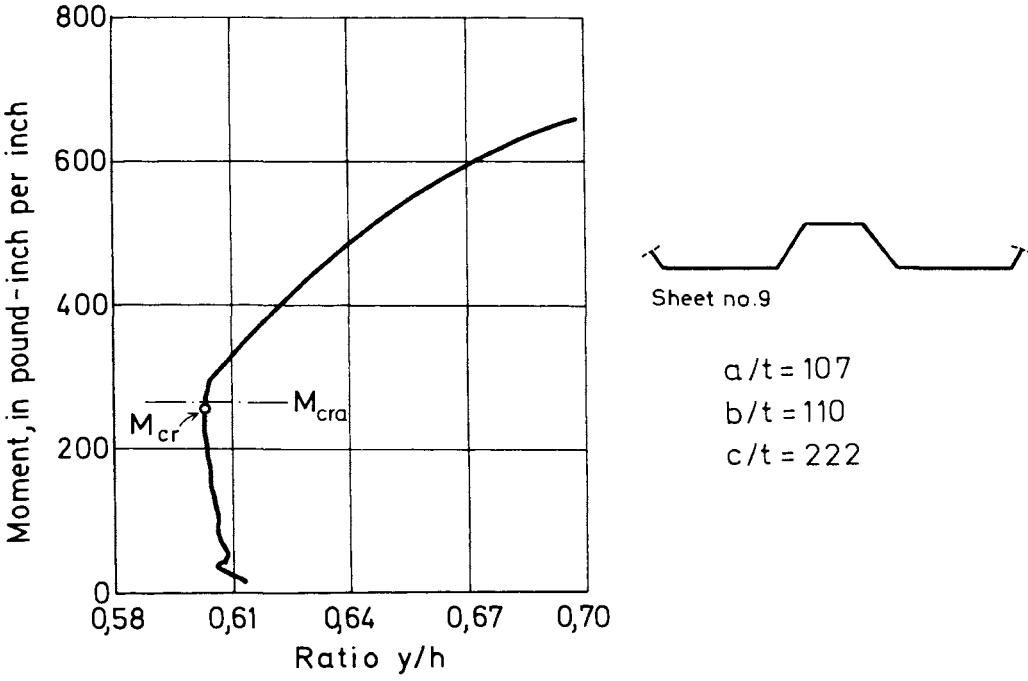

FIG. 6 RELATIVE POSITION OF THE NEUTRAL AXIS, y/h, VERSUS APPLIED MOMENT.
Test No. 9, Ref. 2.
M_{cra} is the theoretical flange buckling load in the plate assembly model.

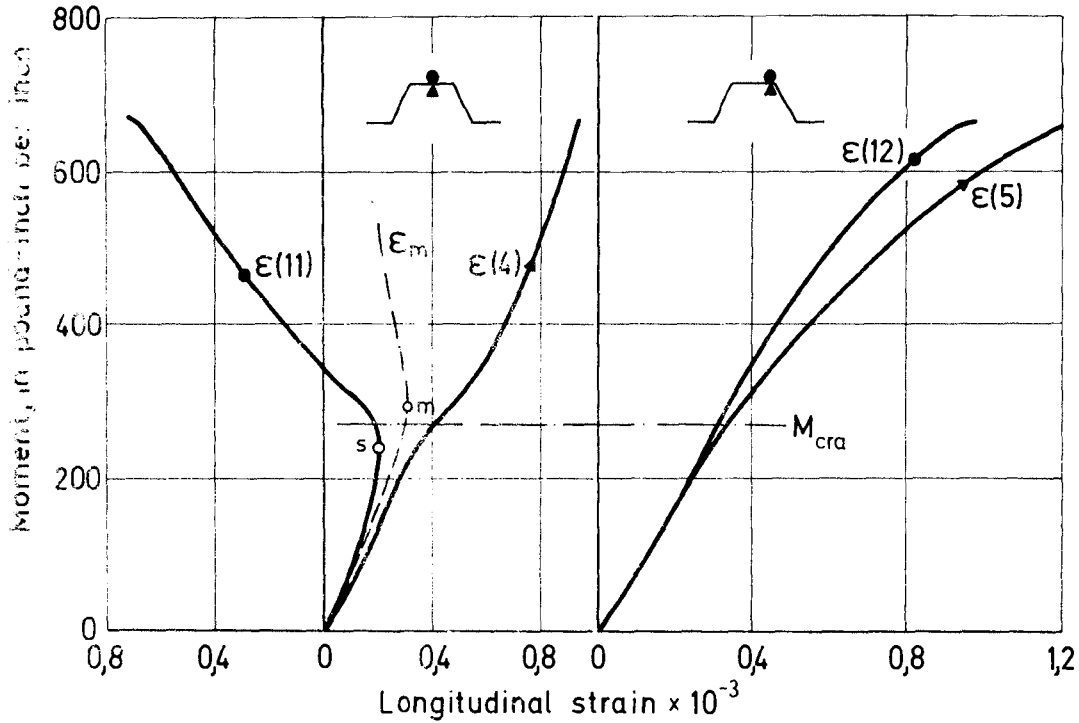

FIG. 7 EXPERIMENTAL LOAD-STRAIN DIAGRAMS FOR COMPRESSION FLANGE.
Test No. 9, Ref. 2.

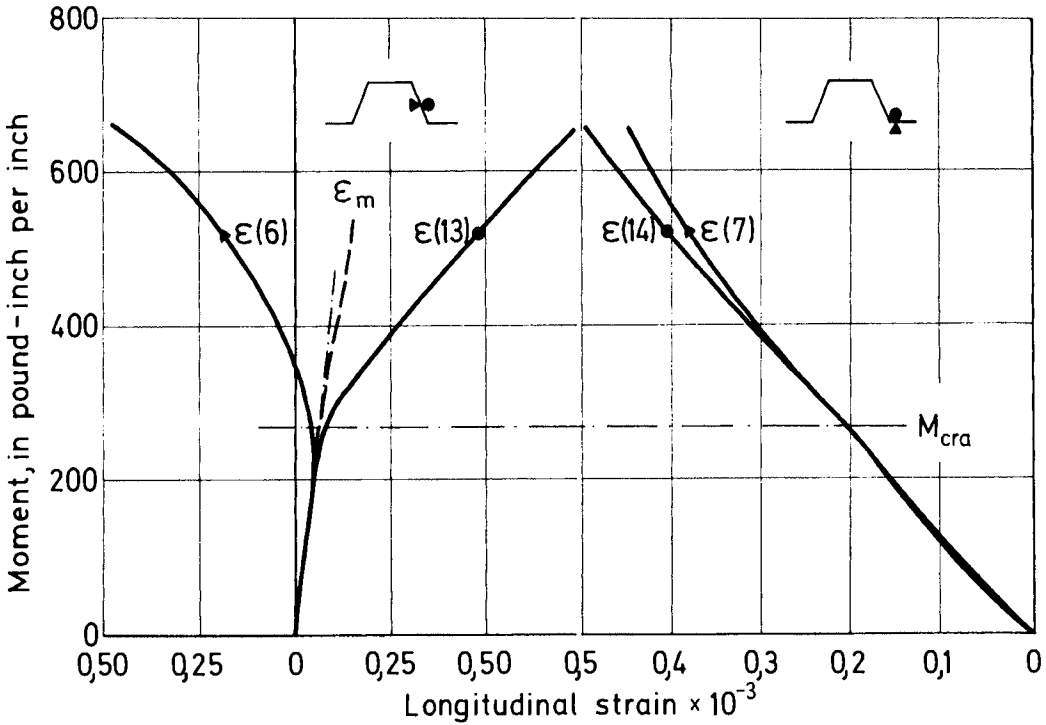

FIG. 8 EXPERIMENTAL LOAD-STRAIN DIAGRAMS FOR WEB AND TENSION FLANGE.
Test No. 9, Ref. 2.

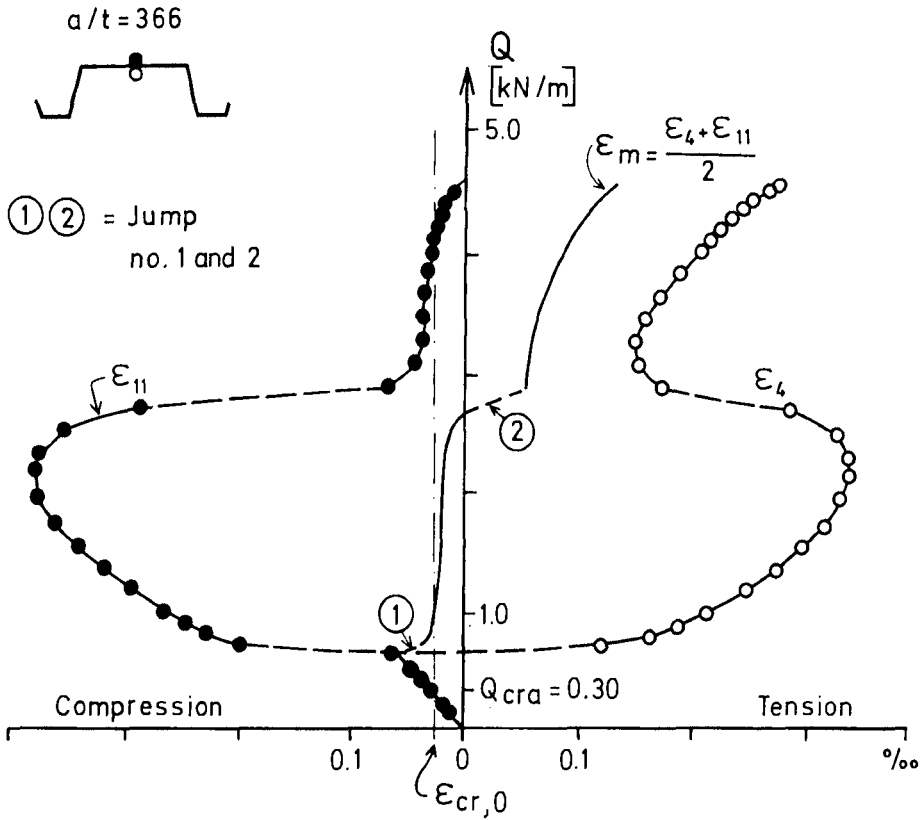

FIG. 9 EXPERIMENTAL LOAD-STRAIN DIAGRAMS AT CENTRE OF WIDE COMPRESSION FLANGE.
Test No. 20, Ref. 2 and Ref. 7.

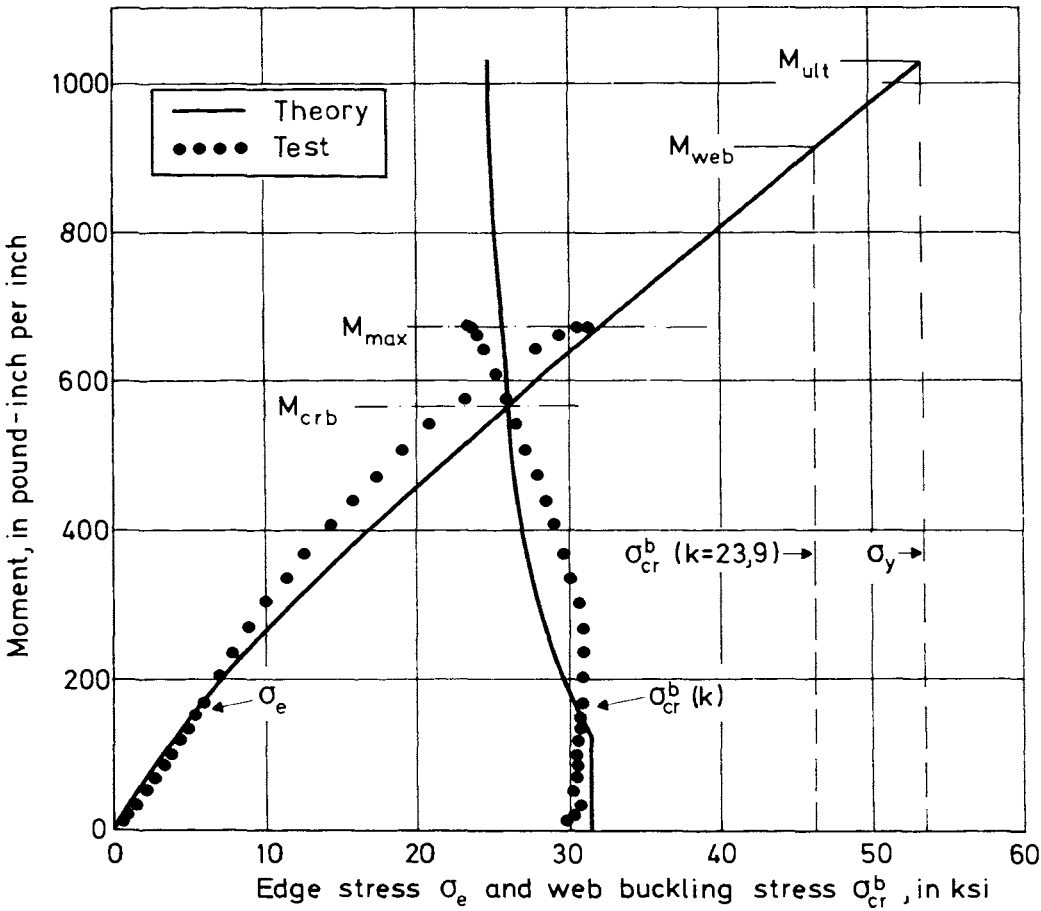

FIG. 10 BENDING MOMENT VERSUS EDGE STRESS σ_e AND WEB BUCKLING STRESS σ_{cr}^{b} RESPECTIVELY. STEEL SHEET TEST No. 9. REF. 2.

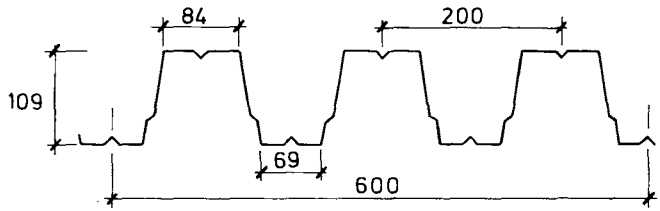

FIG. 11 TRAPEZOIDAL COLD-ROLLED STEEL SHEET WITH INTERMEDIATE FLANGE AND WEB CORRUGATIONS. (PLANNJA TRP 110, Norrbottens Järnverk AB, Luleå, Sweden)